PROCEEDINGS, Twenty-Second Workshop on Geothermal Reservoir Engineering
Stanford University, Stanford, California, January 27-29, 1997
SGP-TR-155

THREE-DIMENSIONAL COMPRESSIONAL- AND SHEAR-WAVE SEISMIC VELOCITY MODELS FOR THE SOUTHEAST GEYSERS GEOTHERMAL FIELD, CALIFORNIA

Ann Kirkpatrick, John E. Peterson Jr., and Ernest L. Majer

E. O. Lawrence Berkeley National Laboratory
Berkeley, California. 94720

ABSTRACT

Three-dimensional compressional- and shear-wave velocity ("Vp" and "Vs," respectively) structure is obtained for the SE Geysers geothermal area from microearthquake arrival-time data. The results indicate a region of high Vp and high Vs in the northwest portion of the area studied, and a low value of VpNs at depths corresponding to the upper part of the steam reservoir. The Vp and Vs anomalies are found to be well-modeled by the predicted seismic signature of the felsite intrusion.

INTRODUCTION

Here we report on the use of microearthquake (MEQ) arrival-time data to determine the three-dimensional (3-d) compressional (P)- and shear (S)- wave velocity ("Vp" and "Vs," respectively) structure at the southeast portion of the Geysers geothermal area (SE Geysers) (Figure 1). An accurate representation of 3-d P- and S-wave velocity structure is necessary for high-quality location of MEQ hypocenters for studies of seismicity patterns and source mechanics, but it is also hoped that the velocity patterns themselves can be related to conditions of interest within the reservoir, such as saturation or pressure.

Previous investigators have focused interpretations of seismic velocity structure at the Geysers on the predicted effects of the degree of saturation on Vp, Vs, and the ratio VpNs (e.g., *O'Connell and Johnson,* 1991; *Romero et al,* 1995; and *Julian et al,* 1996). Low VpNs ratios observed in the steam reservoir have been thought to reflect low Vp caused by a low bulk modulus due to occupation of much of the pore and other void spaces by a vapor rather than liquid phase. It has been theorized, that as steam is extracted from the reservoir and available pore liquid is converted to vapor phase in response to the lowered pressure, that Vp and therefore VpNs are further lowered. Laboratory measurements on Geysers core, however, have shown that while VpNs ratios are indeed lowered as saturated samples are de-saturated, the change is due also, and perhaps primarily, to an increase in Vs *(Boitnott,* 1995, *Boitnott and Boyd,* 1996). This unexpected increase in Vs is thought to be due to an increase in shear modulus as the illite faction in the samples is dried out. The increase in shear modulus counteracts the decrease in bulk modulus with desaturation so that Vp remains relatively unchanged.

We evaluate the results of our arrival-time inversions to determine if these types of seismic signatures in Vp, Vs, and VpNs of core-size samples can be seen in the SE Geysers on the field scale, or if other factors such as lithology or fracture density are more likely to produce the observed velocity patterns.

DATA AND METHOD

In 1993, Lawrence Berkeley National Laboratory and Lawrence Livermore National Labaratory installed a 13-station, 3-component, high frequency (4.5 Hz), digital (480 samples/s) seismic network at the SE Geysers (Figure 2). The network became fully operational in 1994, and 1069 events were detected and located during the first six months of 1994. Of these, 297 events (Figure 2) were chosen to use in the inversion for 3-D P- and S-wave velocity structure using the progressive inversion method of *Thurber* (1983) as modified by *Michelini and McEvilly* (1991). The events were chosen to yield the most even distribution over the study area, with the data having the highest signal-to-noise ratio. The arrival times were picked by visual examination of the seismograms. P-arrivals were picked on vertical components and S-arrivals only on horizontal components. Most P- times were judged accurate to between one and three samples, or .002 to .006 sec., and S-times judged accurate to between 2 and 6 samples (.004 to .012 sec.). The 297 events yielded 2860 P-arrival times (or an average of 10 stations recording a readable P-arrival for each event) and 1637 S-arrival times (an average of 5 readable S-arrival times per event).

The inversion method uses damped least squares to determine the perturbations to an initial estimated

velocity model and to initial estimated hypocentral parameters (location and origin time) which result in lowered travel-time residuals (the difference between the measured arrival times and the arrival times calculated through the current estimate of the velocity model using the current estimate of the hypocentral parameters). Comparable residuals but quite different final velocity models can be obtained using different starting velocity models, so it is important to use the best possible estimate of the 1-d velocity structure as the starting model for the 3-d inversion.

RESULTS AND DISCUSSION

One-Dimensional Model

To get the starting model for the 3-d inversion, the data were first inverted for a 1-d model, constraining the solution to vary only with depth. These results were also dependent upon the choice of a starting model and trials were performed with several different starting models. Two of these starting models are shown in Figure 3. "Start model 1" is based on the 1-d Vp-model that Unocal uses to locate the events detected by their network. It is, in turn, based on the results of *Eberhart-Phillips and Oppenheimer* (1984) in the deeper sections, and the results of a seismic refraction study for the shallower layers *(M. Stark,* pers. comm.). "Start model 2" is based on the 1-D Vp results of *O'Connell and Johnson* (1991) in the north-central area of the Geysers. Performing a suite of inversions using these two starting models and various averages and combinations of them yielded three different 1-d Vp models possessing comparable residuals and resulting in comparable variance reductions. A VpNs ratio of 1.68 was then applied to each of these three Vp models to obtain the Vs values used as starting models in further inversion trials for both 1-d Vp and Vs structure. The ratio 1.68 was chosen because it appears to be about the average value for the SE Geysers portion of the velocity model obtained by *Julian et al* (1996). One resulting Vp and Vs model was superior in terms of residuals and variance reduction and is given in Figure 3. This result, with the modifications discussed below, was used as the starting Vp and Vs model for the 3-d inversion.

An interesting feature of the 1-d results is the low VpNs ratio at all depth levels, with the lowest ratio occurring at an elevation of -0.5 km msl. The top of the steam reservoir varies from approximately 0.0 to -1.0 km msl in this area (Figure 4), so it would appear that the maximum VpNs anomaly is correlated with the upper part of the producing steam reservoir. *O'Connell and Johnson* (1991) also found a low VpNs ratio at depths corresponding to the producing steam reservoir in the north-central Geysers, and *Julian et al's* (1996) recent inversions of USGS, Unocal, and **IRIS** data for 3-d velocity structure over a large area of the central Geysers also found low VpNs ratios corresponding to both the lateral and vertical extent of the steam reservoir. Low VpNs between 1 and 3 km depth below surface was also found at the NW Geysers by *Romero et al* (1995). All of these investigators attributed the low VpNs to undersaturated conditions in the steam reservoir, and indeed, laboratory measurements of Geysers core samples indicate that VpNs is lowered in undersaturated matrix material, as discussed in the previous section. However, comparison of these measurements with seismic inversion results have also indicated that field-scale compliant features, such as joints and fractures, have a much greater effect upon field-scale velocities at these depths than matrix saturation (e.g. *Boitnott,* 1995). It is possible that field-scale bulk and shear moduli are affected by desaturation in the fractures in much the same way that matrix bulk and shear moduli are affected by matrix pore space desaturation, as suggested by *Boitnott and Kirkpatrick* (this issue). It may be that the combined effects of variations in matrix saturation and in fracture properties such as fracture density and fracture saturation, within the reservoir and between the reservoir and the over- and under-lying material, produce the observed anomalies in VpNs.

"Start model 1" was considerably higher in velocity than "Start model 2"; the final results are intermediate between the two models at the shallower levels, but higher than either for the two deepest levels (-1.5 and -2.0 km msl). As can be seen in Figure 2, data is scarce below 2 km depth so the deeper values must be viewed with caution (resolution is discussed more fully in the next section). However, these higher velocities could reflect the fact that the felsite intrusion is almost fully emplaced at these depths in the SE Geysers (Figure 4), while it is generally deeper in the other areas of the Geysers which were the focus of the previous studies.

Three-Dimensional Model

For the 3-d inversion, a horizontal node spacing of 1 km and a vertical node spacing of 0.5 km (the same as used in the 1-d inversion) was used. The inversion geometry is shown in Figure 2. A volume 7 km x 4 km x 2.5 km was imaged. The 1-d Vp and Vs results discussed above were used as the starting model, with the exception that the values for Vs at -1.5 and -2.0 were adjusted to be equal to Vp/1.68.

The results are shown in Figure 5, and are presented as deviations from the average velocity in each layer. The average velocity was computed for each layer using only the better-resolved nodes, defined as

having a spread-function value less than 1.0. The spread function values are shown in Figure **6.** The spread function is a measure of the "resolving width" of the row in the resolution matrix corresponding to a particular node. A perfectly-resolved node would have a resolution-matrix row representing a delta-function, and the resolving-width, or spread, would be zero. Thus lower values in Figure **6** represent the better-defined nodes. As can be seen from Figure **6,** and also from simply considering the ray paths that would result from the hypocenter-station combinations in Figure *2,* the nodes around the edges of the area, and the two deeper nodes, are the worst resolved. The uppermost layer, at 0.5 msl, is also not as well-resolved as the 0.0, -0.5, and -1.0 km msl layers. Differences between Vp- and Vs- resolution result both from differences in number of P-wave paths v.s. S-wave paths, and differences in the paths themselves.

As can be seen in Figure *5,* there are high-velocity anomalies in both P and S in the northwest portion of the area imaged, and an area of low P-velocity slightly northeast of center. The high anomalies are generally more pronounced in Vs than' in Vp, especially in the uppermost two layers, and result in an apparent low VpNs anomaly in the northwest part of the first two layers. The low VpNs ratio at -0.5 km msl, seen in the 1-d results, is preserved in the 3-d inversion, and at this depth extends over most of the area. It must be kept in mind that Vp and Vs are damped separately in the inversion. Choice of damping parameters is largely a trial-and-error procedure, and can have a considerable effect on the magnitude of the variation in the solution from the starting model. The larger Vs variation in the two shallowest layers compared to the Vp variation, and the resulting lateral VpNs patterns, could thus be possibly explained as an artifact of the inversion method, and must be interpreted cautiously.

The felsite intrusion which underlies the Geysers geothermal area intrudes to its maximum elevation in the SE Geysers, in the northwest section of this study area. The intersection of the top of the felsite with each horizontal nodal inversion plane was shown in Figure 4. A comparison of Figure **5** with Figure 4 shows that the Vp and Vs highs at the 0.0, -0.5, and -1.0 km msl layers appear to correlate with the location of the felsite. The felsite is expected to have higher seismic P- and S-velocity than the main greywacke and other metamorphic assemblages into which it is intruded because it is generally less fractured than these units *(Beall and* **Box,** 1992).

Synthetic Test

To test the hypothesis that the felsite intrusion was being imaged in the Vp and Vs results, a synthetic test was conducted. The felsite body was parameterized by assigning Vp and Vs values to the inversion nodes enclosed by the felsite contours, of *5%* greater than the background nodes, for each layer (Figure 7). P- and S-waves were traced through this synthetic velocity structure, and synthetic arrival times computed for the same event-station pairs possessed by the real data. Then these synthetic arrival times were inverted to see if the original synthetic velocity structure could be recovered. This type of test provides a method to assess the ability of the data at hand to resolve the postulated structure.

As can be seen from Figure 7, the inverted synthetic data velocity model recovers the gross features of the synthetic structure very well. However, there is some "smearing" of the high-velocity values to neighboring nodes (both laterally and vertically), and some reductions in background velocity below the true synthetic values. Even so, these results indicate that if there is a velocity contrast of *+5%* between the felsite and the intruded rock, our data is capable of imaging it. It should be mentioned, however, that a more complete test would add random noise to the computed arrival times to simulate picking errors, and would be expected to smear the final model even further.

The question of whether the synthetic data inversion results match the real data inversion results is a separate one, and is addressed in Figure 8. Here the recovered synthetic model is plotted as deviations from the average velocity in each layer, rather than as deviation from the background velocity as in Figure 7. This is how the inversion results of the real data were presented in Figure *5.* Direct comparison of Figures 8 and *5* shows that the real data inversion results match the synthetic data inversion results to a remarkable degree, in both Vp and Vs, within the well-resolved portions. When the synthetic results are plotted in this fashion, the low-velocity "halos" around the high-velocity body are more clearly seen. This artifact of the inversion method could account for many of the low velocities surrounding the high-velocity anomalies in the real inversion results. Alternatively, there could actually be a zone of anomalously low velocity surrounding the felsite intrusion, caused by high-temperature thermal brecciation as the pluton was emplaced (e.g. *Hulen et al*, 1993). These low-velocity zones should also be investigated to see if they correlate with other reservoir parameters such as pressure, flow rates, and seismicity rates.

Some of the real-data high velocities at the 0.5 and 0.0 msl levels, in areas that are known to not be comprised of felsite, could also be artifacts of the inversion method (e.g. "smearing out" of real high-

velocity at neighboring nodes). However, some of these anomalies are so strong, especially in Vs in the upper-most layer, that they also should be investigated further.

SUMMARY AND CONCLUSIONS

The one-dimensional inversion results show low VpNs ratios throughout the entire depth range of the area imaged. The lowest ratio correlates with the upper part of the steam reservoir.

The three-dimensional inversion results show lateral variations in Vp and Vs of up to +/- 6%. Areas of high P-velocity generally correlate with areas of high S-velocity, and areas of low P-velocity also generally correlate with areas of low S-velocity. This is not what would be expected if the lateral variations were due to variations in reservoir or matrix saturation, as the laboratory measurements show that degree of saturation affects P- and S-velocities in opposite ways in Geysers core material. Additionally, work by ***Boitnott and Kirkpatrick*** (this issue), has demonstrated that lateral variations in matrix saturation can not produce the range of variation in field-scale VpNs observed at the shallower depth levels. Their application of a model incorporating both matrix and field-scale compliant feature effects to the NW Geysers results of ***Romero et al*** (1996) required lateral variations in properties of the field-scale compliant features to reproduce the seismic inversion results. This is consistent with the results of our synthetic test, which show that the 3-D Vp and Vs seismic inversion results for the SE Geysers could reflect lateral velocity variations caused by lateral variations in fracture density between the felsite and the intruded greywacke and other Franciscan rocks.

ACKNOWLEDGMENTS

This work was supported by the Assistant Secretary for Energy Efficiency and Renewable Energy, Geothermal Division, under contract No DE-AC03-76F00098. The authors would like to thank Unocal, Calpine, and NCPA for their cooperation and input on this project. Particular thanks are given to Joe Beall of Calpine, Bill Cumming of Unocal, and Bill Smith of NCPA. Greg Boinott, Tom McEvilly, and Roland Gritto are also thanked for many stimulating discussions of the results.

REFERENCES

Beall, J. J., and W. T. Box, Jr. (1992), The nature of steam-bearing fractures in the south Geysers reservoir, Geotherm. Resourc. Counc. Special Report No. 17, 69-75.

Boitnott, G. N. (1995), Laboratory measurements on reservoir rocks from the Geysers geothermal field, Proc. 20th Workshop on Geotherm. Reservoir Engineering, Stanford University, 107-114.

Boitnott, G. N., and A. Kirkpatrick, Interpretation of field seismic tomography at the Geysers geothermal field, California, this issue.

Eberhart-Phillips, D., and D. H. Oppenheimer (1984), Induced seismicity in the Geysers geothermal area, California, J. Geophys. Res. **89,** 1191-1207

Field Operators (1992), Map of the top of the steam reservoir at the Geysers, and Map of the top of the felsite at the Geysers, Geotherm. Resourc. Counc. Special Report No. 17.

Hulen, J. B., and D. L. Nielson (1993), Interim report on geology and hydrothermal alteration of the Geysers felsite, northwestern California, GRC Trans., 17, 249-258.

Julian, B. R., A. Ross, G. R. Foulger, and J. R. Evans (1996), Threedimensional seismic image of a geothermal reservoir: The Geysers, California, Geophys. Res. Let. 23, 685-688.

Michelini, A., and T. V. McEvilly (1991), Seismological investigations at Parkfield: I. Simultaneous inversion for velocity structure and hypocenters using cubic b-spines parameterization, Bull. Seismol. Soc. Am. 81, 524-552.

O'Connell, D. R., and L. R, Johnson (1991), Progressive inversion for hypocenters and P wave and S wave velocity structure: Application to the Geysers, California, geothermal field, J. Geophys. Res. 96, 6623-6236.

Romero, **A.** E., T. V. McEvilly, **E.** L. Majer, and D. Vasco (1995), Characterization **of** the geothermal system beneath the Northwest Geysers steam field, California, from seismicity and velocity patterns, Geothermics, 24, 471-487.

Thurber, D. H. (1983), Earthquake locations and three-dimensional crustal structure in the Coyote Lake area, Central California, J. Geophys. Res. 88, 8826-8236.

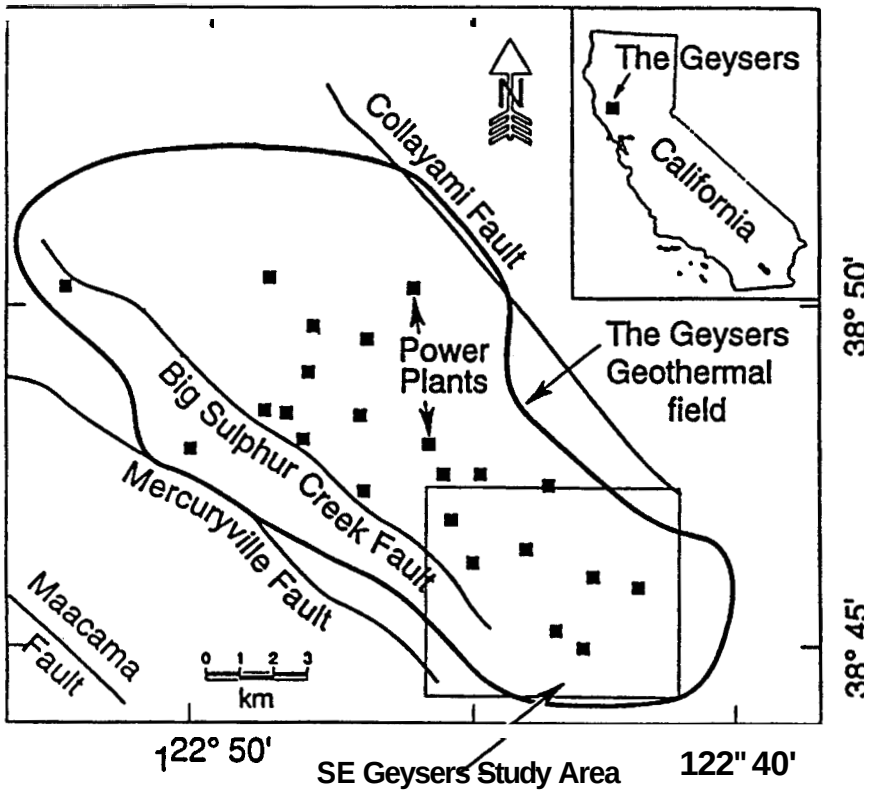

Figure 1. Location of the SE Geysers study area. The boxed area is shown in detail in Figure 2.

(a)

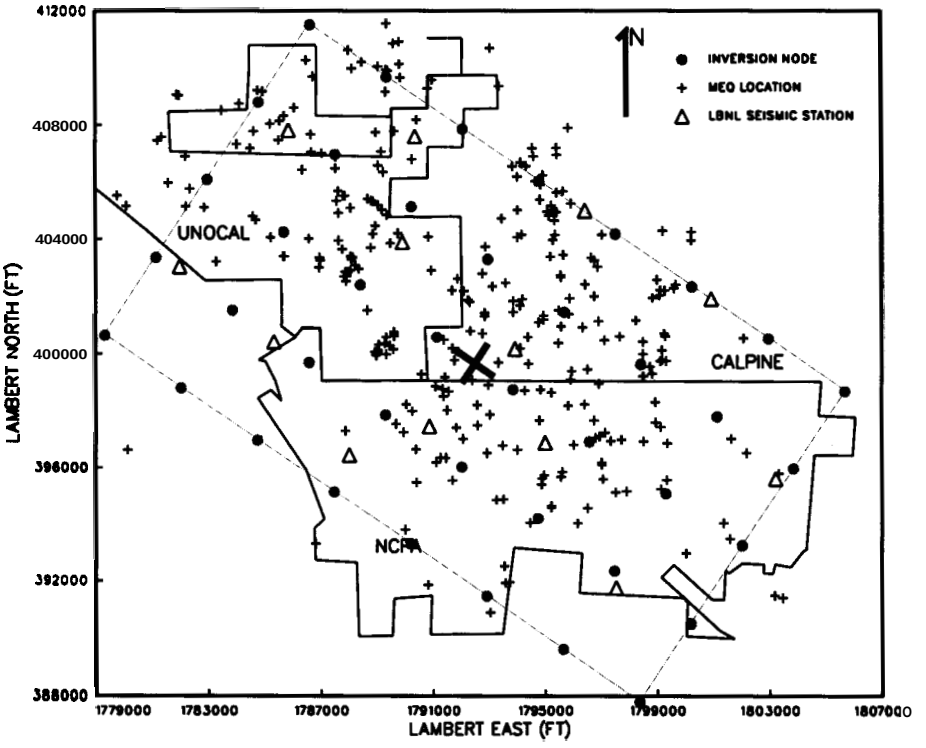

(b)

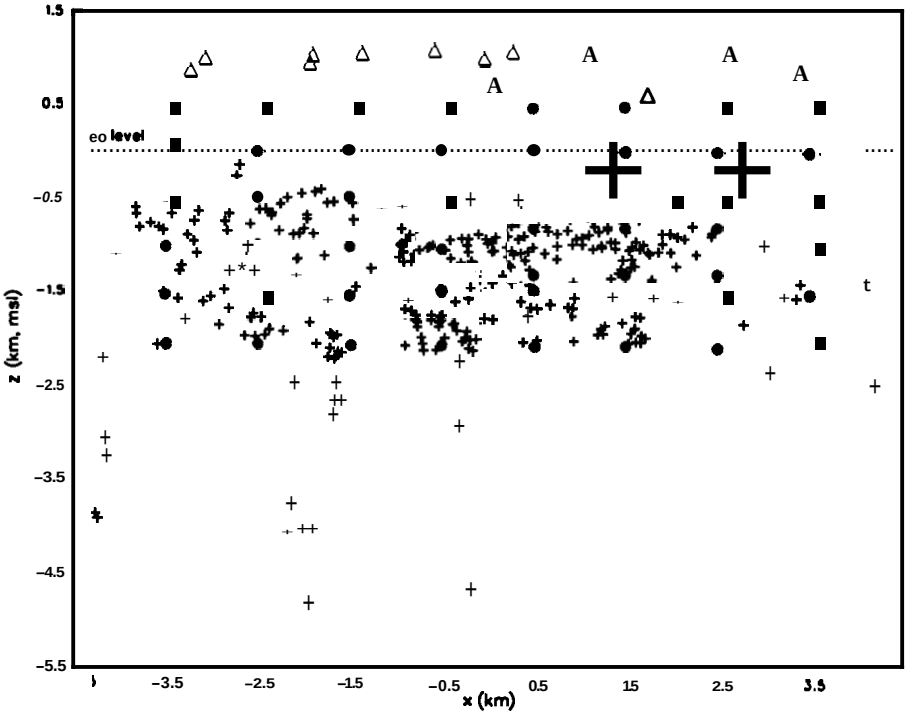

Figure 2. a) Location of the stations of the LBNL Seismic Network, inversion nodes, and MEQs used in the 1-D and 3-D inversions. The black cross denotes the center of the inversion grid and the directions of the x and y axes (the x-axis is rotated 34° clockwise from e-w). The rectangle defined by the inversion nodes is shown in the subsequent Figures 4 through 8. b) Projection of MEQs, nodes, and stations onto the vertical plane along the x-axis.

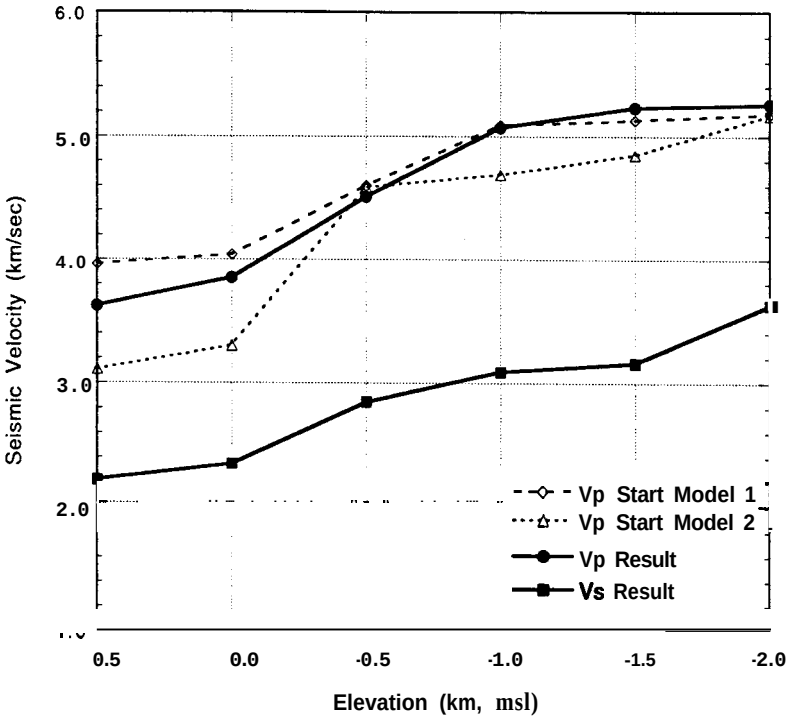

(a)

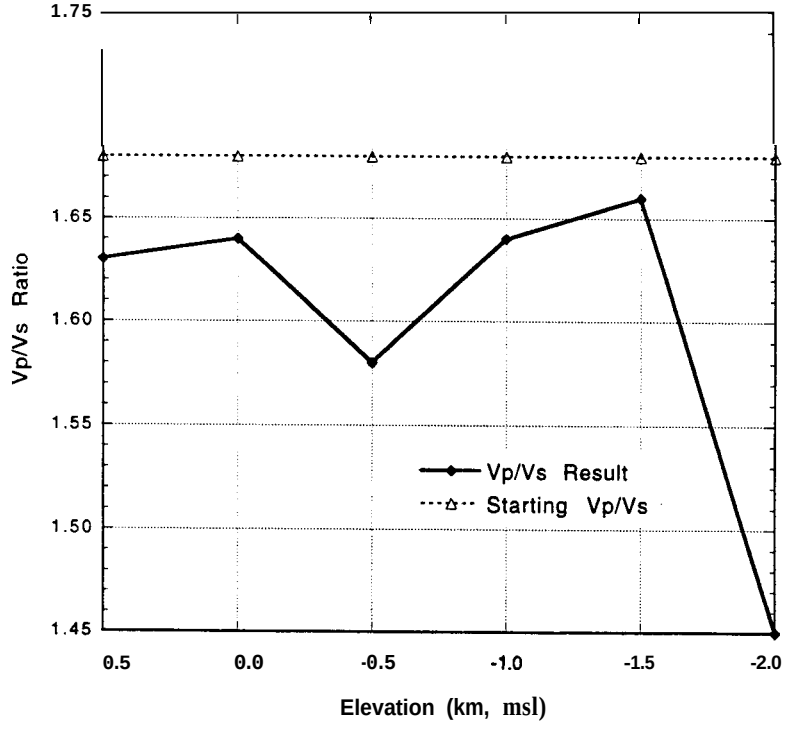

(b)

Figure **3.** One-dimensional inversion starting models and results. a) **Vp** and Vs. b) **VpNs** ratio.

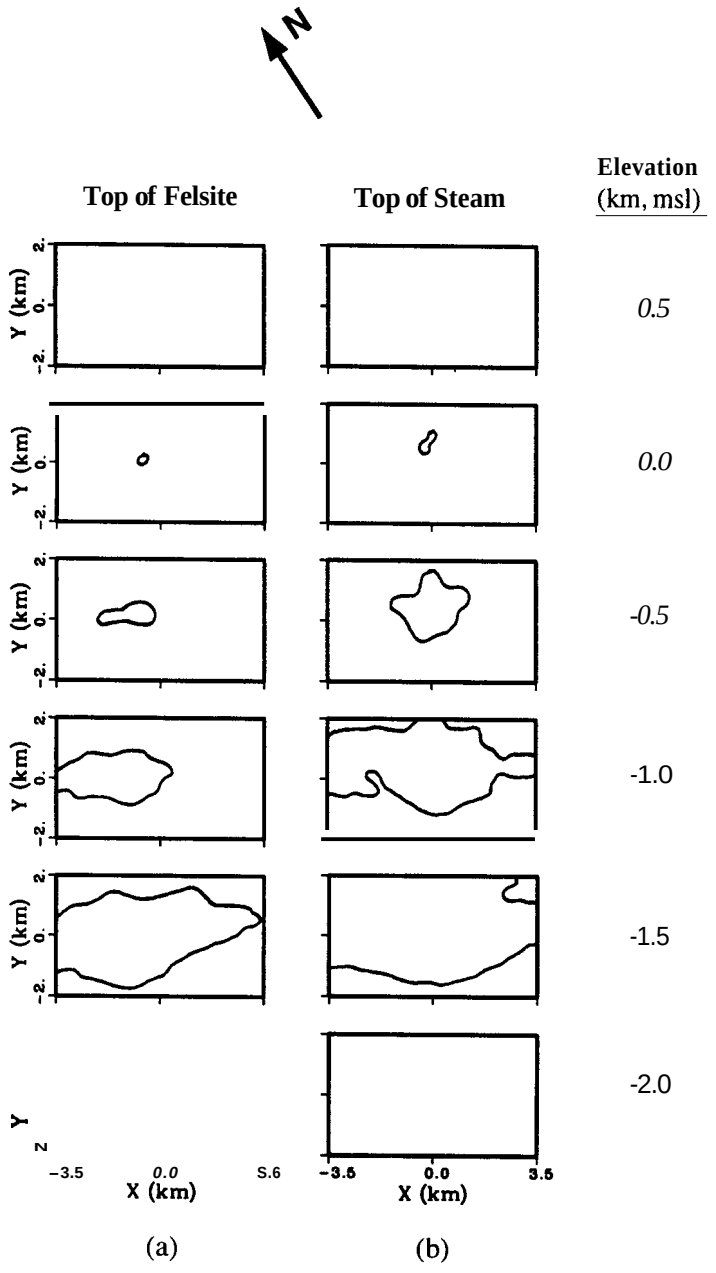

Figure 4. Intersection of a) top of **felsite intrusion and** b) **top of steam reservoir, with the horizontal plane at each depth node of the inversions (see Figure 2). Derived from data compiled by the *Field Operators* (1992).**

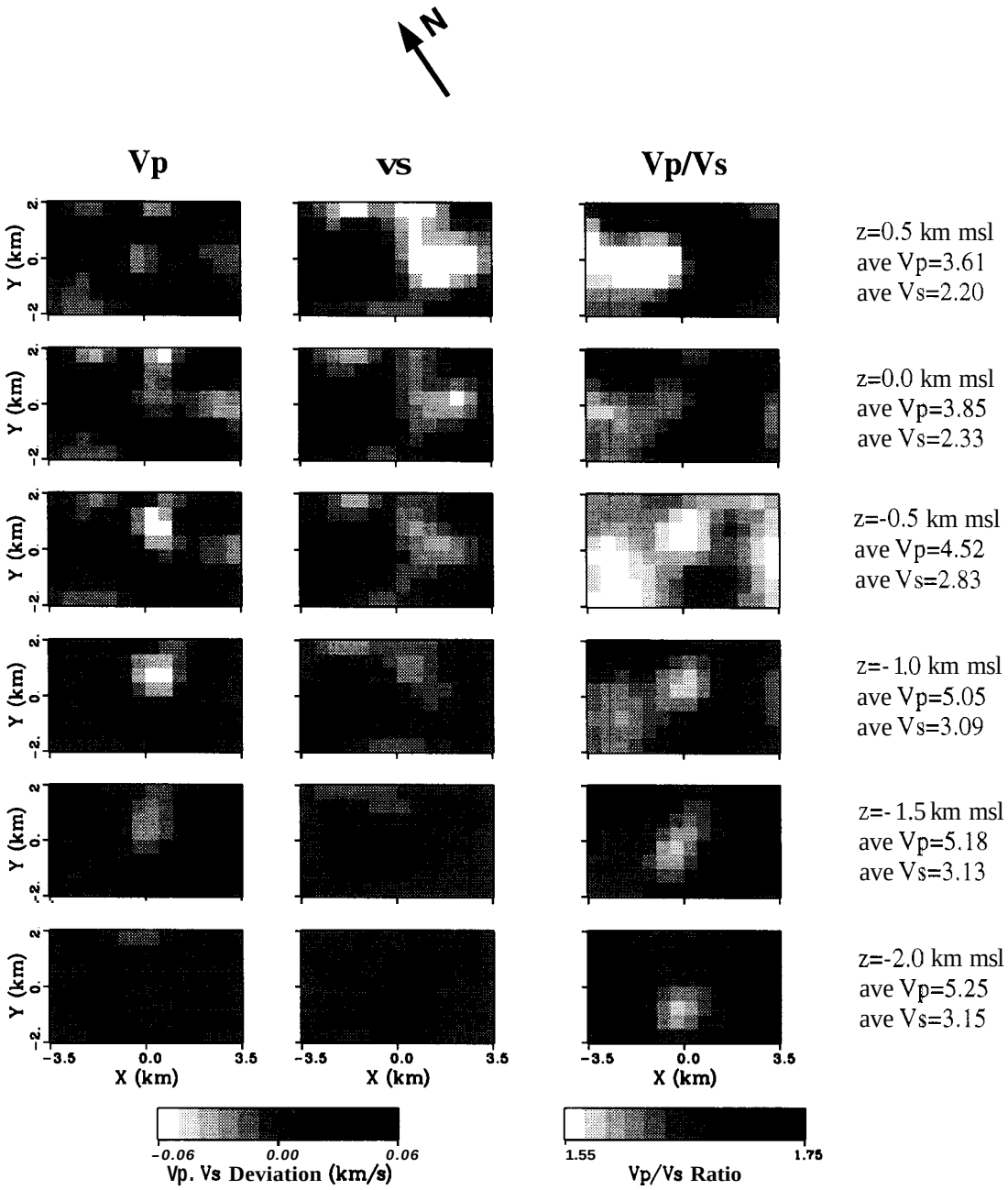

Figure 5. Three-dimensional velocity inversion results. Horizontal slices at each of the depth nodes are presented (see Figure 2). The P- and S-velocities are plotted in terms of their deviations from the average P- and S-velocity at each depth, given to the right of the slices.

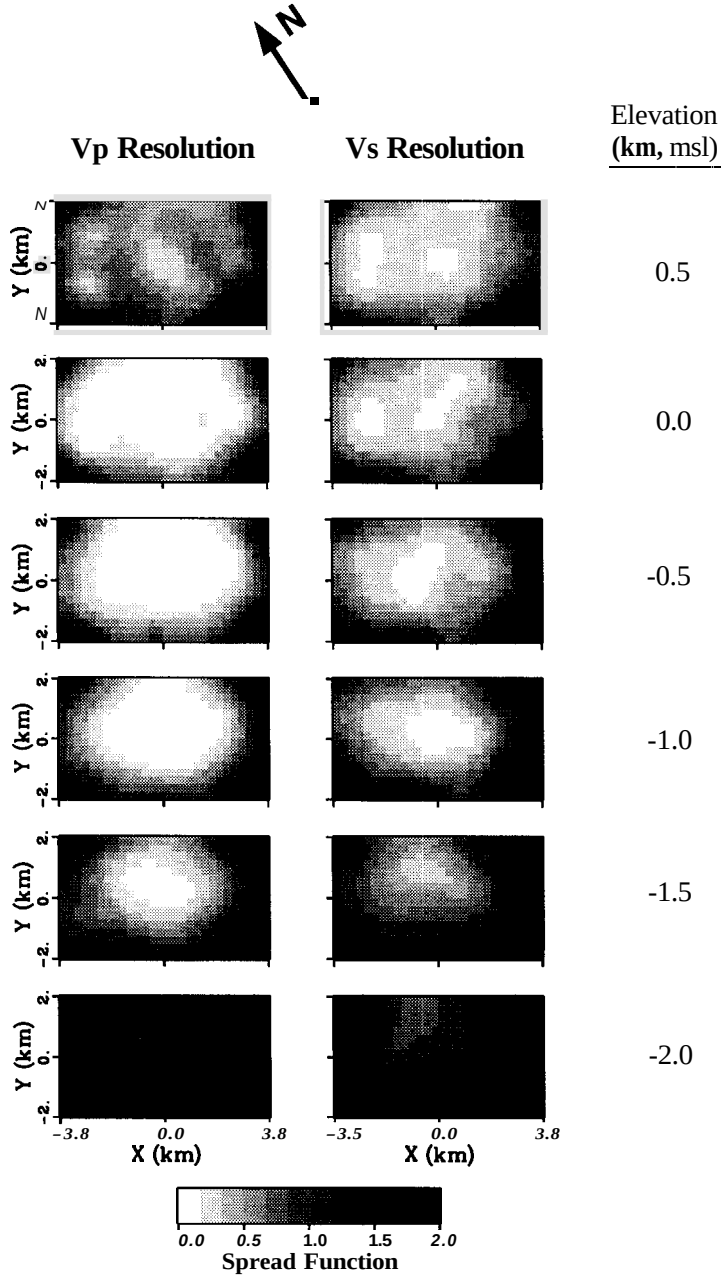

Figure 6. Vp and Vs model resolution, for the results presented in Figure 5.

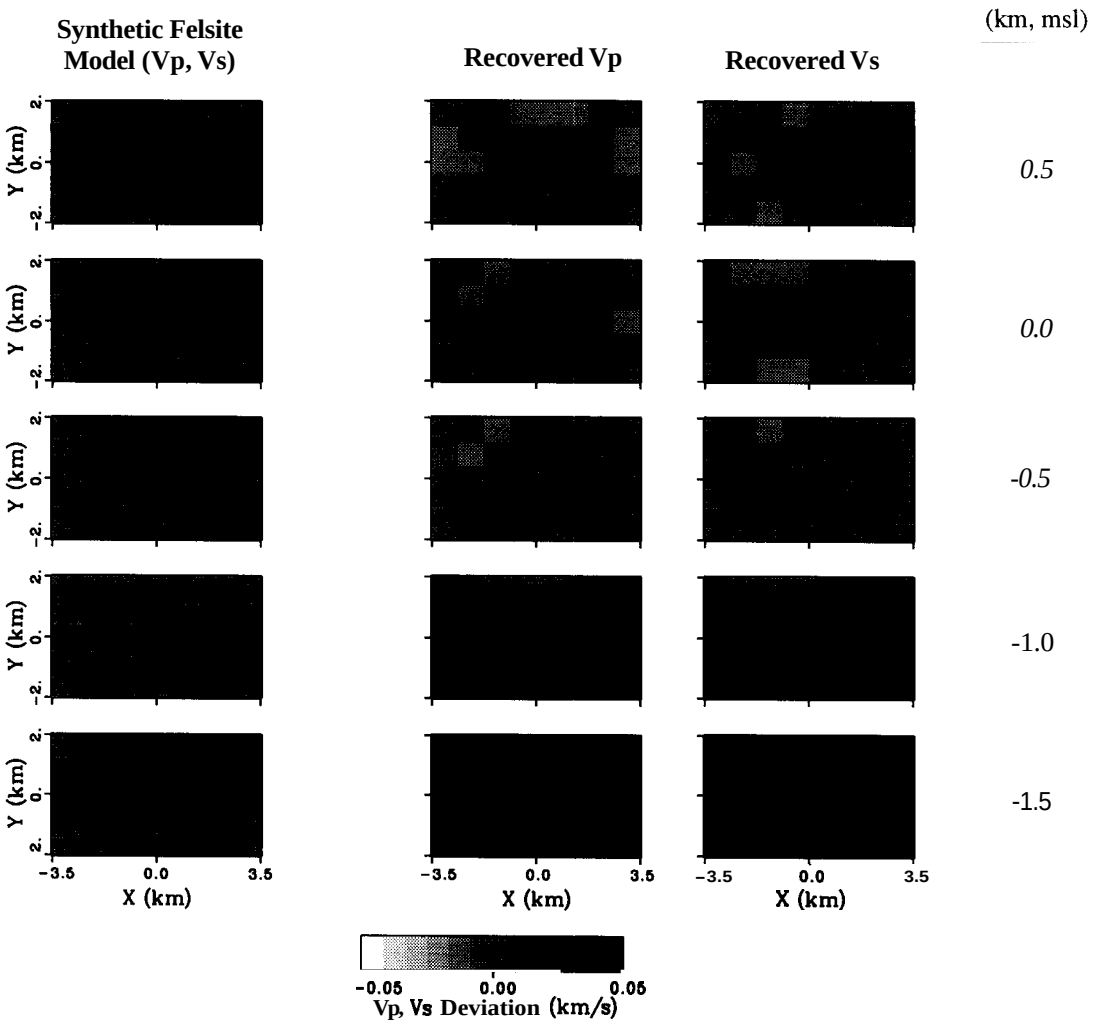

Synthetic model: "background" velocities / "felsite" velocities:

elev.	Vp	Vs
0.5	*3.50* / none	2.10 / none
0.0	*3.15 13.94*	*2.23 12.35*
-0.5	*4.40 14.62*	*2.62* / 2.75
-1.0	*4.85 15.09*	*2.89 13.03*
-1.5	*5.00* / 5.25	*2.98 13.13*
-2.0	none *15.35*	none / 3.18

Figure 7. Synthetic velocity model, representing a parameterization of a high-velocity body corresponding to the location of the felsite (shown in Figure **4)** used to calculate the synthetic arrival times; and the recovered Vp and **Vs** models from the inversion of the synthetic arrival times. All models are plotted as deviations from the synthetic model "background" velocity at each depth slice, given in the accompanying table.

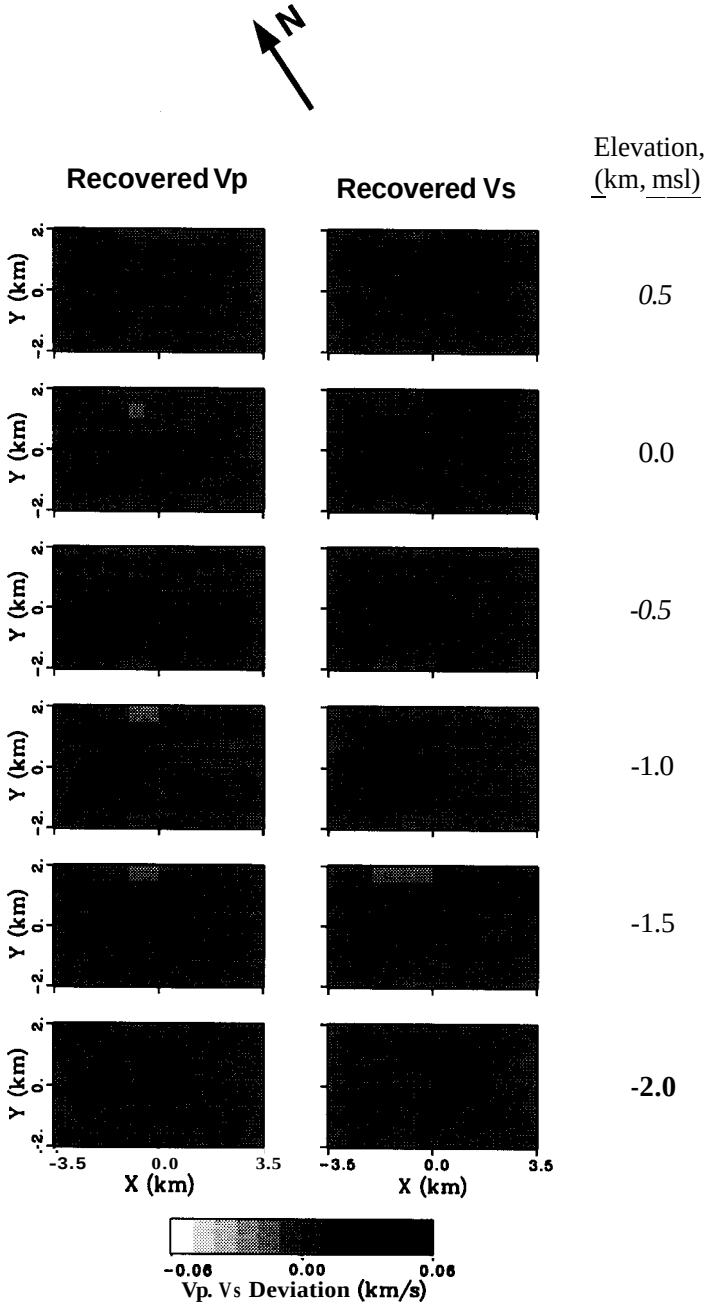

Figure 8. Same as Figure 7, recovered Vp and recovered Vs, except plotted as deviations from the average recovered P- and S-velocities at each depth slice. Compare with Figure 5.